Analysis of host factor networks during hepatitis B virus infection in primary human hepatocytes

Suhyun Hwangbo[1†], Gahee Kim[2,4†], Yongwook Choi[2], Yong Kwang Park[2], Songmee Bae[2], Jae Yong Ryu[3†] and Wonhee Hur[2*†]

Abstract

Background Chronic hepatitis B virus (HBV) infection affects around 250 million people worldwide, causing approximately 887,000 deaths annually, primarily owing to cirrhosis and hepatocellular carcinoma (HCC). The current approved treatments for chronic HBV infection, such as interferon and nucleos(t)ide analogs, have certain limitations as they cannot completely eradicate covalently closed circular DNA (cccDNA). Considering that HBV replication relies on host transcription factors, focusing on host factors in the HBV genome may provide insights into new therapeutic targets against HBV. Therefore, understanding the mechanisms underlying viral persistence and hepatocyte pathogenesis, along with the associated host factors, is crucial. In this study, we investigated novel therapeutic targets for HBV infection by identifying gene and pathway networks involved in HBV replication in primary human hepatocytes (PHHs). Importantly, our study utilized cultured primary hepatocytes, allowing transcriptomic profiling in a biologically relevant context and enabling the investigation of early HBV-mediated effects.

Methods PHHs were infected with HBV virion particles derived from HepAD38 cells at 80 HBV genome equivalents per cell (Geq/cell). For transcriptomic sequencing, PHHs were harvested 1, 2-, 3-, 5-, and 7 days post-infection (dpi). After preparing the libraries, clustering and sequencing were conducted to generate RNA-sequencing data. This data was processed using Bioinformatics tools and software to analyze DEGs and obtain statistically significant results. Furthermore, qRT-PCR was performed to validate the RNA-sequencing results, ensuring consistent findings.

Results We observed significant alterations in the expression patterns of 149 genes from days 1 to 7 following HBV infection ($R^2 > 0.7$, $q < 0.05$). Functional analysis of these genes identified RNA-binding proteins involved in mRNA metabolism and the regulation of alternative splicing during HBV infection. Results from qRT-PCR experiments and the analysis of two validation datasets suggest that RBM14 and RPL28 may serve as potential biomarkers for HBV-associated HCC.

Conclusions Transcriptome analysis of gene expression changes during HBV infection in PHHs provided valuable insights into chronic HBV infection. Additionally, understanding the functional involvement of host factor networks

†Suhyun Hwangbo and Gahee Kim contributed equally to this work and share first authorship.

†Jae Yong Ryu and Wonhee Hur contributed equally to this work and share last authorship.

*Correspondence:
Wonhee Hur
wonhee.her@gmail.com
Full list of author information is available at the end of the article

Hwangbo *et al. Virology Journal*   (2024) 21:170

Page 2 of 12

in the molecular mechanisms of HBV replication and transcription may facilitate the development of novel strategies for HBV treatment.

Keywords Hepatitis B virus, Primary human hepatocytes, Transcriptome analysis, RNA-binding proteins

Background

Hepatitis B virus (HBV), a prototypical member of the Hepadnaviridae family, is responsible for inducing acute and chronic hepatitis B, cirrhosis, and hepatocellular carcinoma (HCC) [1]. Despite the availability of safe and highly effective vaccines against HBV, chronic infection remains a significant public health challenge, affecting an estimated 296 million individuals worldwide. It is the second-leading cause of cancer-related mortality worldwide [2]. HBV is an enveloped DNA virus that contains a small, partially double-stranded 3.2 kb DNA genome, or relaxed circular DNA (rcDNA). The rcDNA transforms into covalently closed circular DNA (cccDNA), serving as a template for viral transcription. cccDNA persists within the nuclei of infected hepatocytes in an episomal state via the intervention of cellular enzymes [3]. Current treatments include nucleos(t)ide analogs (NAs), such as tenofovir or entecavir, which effectively target viral reverse transcriptase activity and reduce viral replication. However, the challenge persists as these treatments do not directly eradicate cccDNA, a pivotal obstacle to achieving a complete virological or sterilizing cure for HBV infection.

The viral transcription produces multiple-length viral RNAs (3.5, 2.4, 2.1, and 0.7 kb) under the control of four viral promoters and two enhancers. Additionally, numerous host cellular transcription factors, such as nuclear receptors and hepatocyte-enriched and ubiquitous transcription factors, participate in the HBV life cycle [4]. Recent reports have highlighted the biological significance of HBV RNA regulation, potentially impacting splicing regulation in a cell type-specific manner [5]. Therefore, a more extensive exploration is needed to understand the biological significance of HBV RNA regulation in hepatocytes, encompassing viral replication, host range, and intricate regulatory mechanisms governing post-transcriptional processing events within the HBV life cycle. Furthermore, understanding the multitude of host factors involved in the HBV life cycle holds promise for uncovering insights guiding the discovery of anti-HBV therapies, focusing on drugs targeting cellular factors.

In this study, we performed RNA-sequencing (RNA-seq) experiment to identify differentially expressed and co-regulated genes in HBV-infected primary human hepatocytes (PHHs). Additionally, to validate our transcriptome data analysis, we compared it with eligible HBV gene expression datasets collected from the public repository Gene Expression Omnibus (GEO). Using this approach, we aim to identify the specific gene expression patterns that could serve as an accurate clinical tool for predicting prognosis and adjuvant therapy responses in HBV infection.

Materials and methods

Cell culture

HepAD38 cells were described in our previous studied [6]. Cells were cultured with or without 5 μg/ml tetracycline (Sigma-Aldrich, St Louis, MO, USA) in Dulbecco's modified Eagle's medium (DMEM)/F-12 (Gibco, Grand Island, NY, USA) supplemented with 10% fetal bovine serum (FBS, Gibco) and 1% penicillin–streptomycin (Gibco) at 37 °C under a humidified atmosphere containing 5% CO_2. Cultured HepAD38 cells were used to produce an HBV inoculum for infection experiments as previously described [6]. PHHs were purchased from Corning (Tewksbury, MA, USA) and maintained in the hepatocyte-specific medium (Corning) with 0.01 μg/mL EGF according to the manufacturer recommendations.

HBV production and infection

For the infection experiments, the HBV inoculum was prepared from freshly collected supernatants of HepAD38 cells as described previously [6]. The titer of the HBV solution was adjusted to 5×10^8 viral genome equivalents (GEq) per mL. PHHs (8×10^5 cells/well) were seeded onto six-well plates coated with collagen I (Gibco) and were inoculated with 80 GEq/cell of HBV in the presence of 4% PEG 8000 (Sigma). After inoculum removal and washing, the cells were incubated in fresh medium. The culture medium was collected and replaced every two days.

Detection of HBsAg and HBeAg

The levels of HBV surface antigen (HBsAg) and HBV e antigen (HBeAg) in the culture medium were determined using an ELISA kit (Wantai Bio-Pharm, Beijing, China) according to the manufacturer's instructions. The absorbance was measured at 450 nm using a spectrophotometer (Synergy H1; BioTek, Winooski, VT, USA). All experiments were performed a minimum of three times.

Quantitative real-time PCR analysis of intracellular HBV DNA

Total genomic DNA was extracted from intracellular HBV rcDNA using a QIAamp DNA Mini Kit (Qiagen, Venlo, Netherlands) according to the manufacturer's instructions. To assess HBV rcDNA levels, quantitative real-time PCR (qRT-PCR) was performed using a Power SYBR green PCR master mix (Applied Biosystems, Warrington, UK) with primers for HBV rcDNA and amplified using the QuantStudio 3.0 program (Applied Biosystems). The primer pairs for HBV DNA were forward primer (nt 256 to 274): 5′-CTCGTGGTGGAC TTCTCTC-3′; and reverse primer (nt 404 to 421): 5′-CTGCAGGATGAAGAGGAA-3′. Relative gene expression levels were normalized against those of β-actin.

RNA-sequencing data generation and analysis

Total RNA was extracted using the TRIzol reagent (Invitrogen, CA, USA) according to the manufacturer's instructions. Isolated RNA was evaluated using an Agilent RNA 6000 Pico kit (Agilent, Santa Clara, CA, USA), and the concentration was measured using a BioPhotometer® spectrophotometer (Eppendorf, Hamburg, Germany). RNA samples with an absorbance ratio at 260/280 nm between 1.8 and 2.0 and structural integrity verified before being used in the sequencing library preparation. A cDNA library was generated using the QIAseq FX Single Cell RNA Library Kit (Qiagen) according to the manufacturer's protocol. In this protocol polyA-selected mRNA was converted in cDNA, and then enzymatic fragmentation (incubation time for "fragment size = 200–500 bp" was used) and library preparation were performed using 1 μg cDNA. The cDNA concentration was measured using the LightCycle qPCR (Roche, Penz Agilent High Sensitivity D5000 ScreenTape System berg, Germany), and the size of library was checked using an Agilent High Sensitivity D5000 ScreenTape System (Santa Clara, CA). RNA-seq was conducted by GnCBio (Daejeon, Korea) using HiSeq X (Illumina, CA, USA), as previously reported [7–9]. Low-quality sequence reads from the raw sequence data were filtered using Trim Galore software (https://github.com/FelixKrueg er/TrimGalore). High-quality sequence reads with a base quality > 30 and length > 50 were selected and mapped to the Homo sapiens reference genome using the Bowtie2 aligner tool [10]. These preprocessing procedures were performed for both HBV-infected and HBV-uninfected PHH samples. Differential expression analysis was conducted between the two groups (HBV-infected and uninfected PHHs) using read count data (See Additional file 1).

In this study, we focused on identifying protein-coding genes related to pathogenesis, and 17,613 protein-coding genes were analyzed. Each gene in the RNA-seq data was measured on days 3, 5, and 7 after HBV infection. For each group, measurements per gene were fitted to a linear regression model. $R^2 > 0.7$ and false discovery rate (FDR)-rate-adjusted *p*-values (i.e., q-values) < 0.05 were used as significance thresholds to select genes showing dynamic changes. In addition to within-group comparisons, between-group comparisons were performed using the Wilcoxon rank-sum test at a significance level of 0.05.

Dataset collection on HBV-infected primary human hepatocytes

To prevent the selection of candidate genes specific to the dataset, validation analysis was carried out using the GSE72068 dataset with a study design similar to ours [11]. The GSE72068 dataset contains microarray expression profiling data showing the gene expression response at various time points (i.e., 4 and 8 h and 1, 6, and 12 days) in HBV-infected PHHs. Among the 18,036 protein-coding genes identified in the GSE72068 dataset, 13,862 overlapped with the those in main dataset generated through RNA-Seq experiments in this study. The same statistical methods used to analyze the main dataset were also applied in the validation analysis.

The GSE25097 dataset was used to identify candidate genes as potential biomarkers for HBV-associated HCC. The GSE25097 dataset is a microarray expression profile designed to identify prognostic genetic markers between 268 HCC tumor samples and 6 healthy liver samples. Among the 18,076 protein-coding genes identified in the GSE25097 dataset, 14,143 genes overlapped with the main dataset used in this study. Comparison of the expression levels between HCC and healthy samples was performed using the Wilcoxon rank-sum test.

Furthermore, to gain insight into the mechanisms of potential biomarkers, we performed a functional enrichment analysis using the Database for Annotation, Visualization, and Integrated Discovery (DAVID) [12].

Statistical analysis

The data are expressed as the mean ± standard deviation. Statistical analysis was performed using the unpaired *t* test (GraphPad Prism 8) to determine statistically significant differences between groups. *$p < 0.05$, **$p < 0.01$, ***$p < 0.001$, and ****$p < 1 \times 10^{-15}$ were considered statistically significant.

Hwangbo *et al. Virology Journal*   (2024) 21:170

Page 4 of 12

Results

Establishment and characteristics of HBV-infected primary human hepatocytes

PHHs were infected with HBV particles collected from HepAD38 supernatant. Successful HBV infection was observed over 7 days, as confirmed by the detection of secreted HBV antigens (HBsAg and HBeAg) and intracellular HBV rcDNA at the indicated time points (Fig. 1A). As shown in Fig. 1B, the levels of HBsAg and HBeAg were found to plateau in HBV-infected cells at approximately 7 days post-infection (dpi). Next, intracellular HBV rcDNA was detected using qRT-PCR (Fig. 1C). The expression of HBV rcDNA increased continuously until 7 dpi. Therefore, PHH infected with HBV constitutes an effective model for studying the cellular effects of post-infection stages of the HBV life cycle. Subsequently, samples were collected at these time points and subjected to RNA-seq analysis.

Changes in gene expression patterns after HBV infection in primary human hepatocytes

To comprehensively identify host gene expression changes in HBV-infected PHHs, we analyzed the dynamic alterations in gene expression patterns following HBV infection. We observed significant alterations in the expression patterns of 149 genes for 7 dpi ($R^2 > 0.7$, $q < 0.05$; Fig. 2A). Among these genes, the expression of a majority of 141 genes (95%; Fig. 2B) showed a decreasing trend over time, whereas a smaller subset of 8 genes (5%; Fig. 2C) exhibited an increasing pattern. The rate
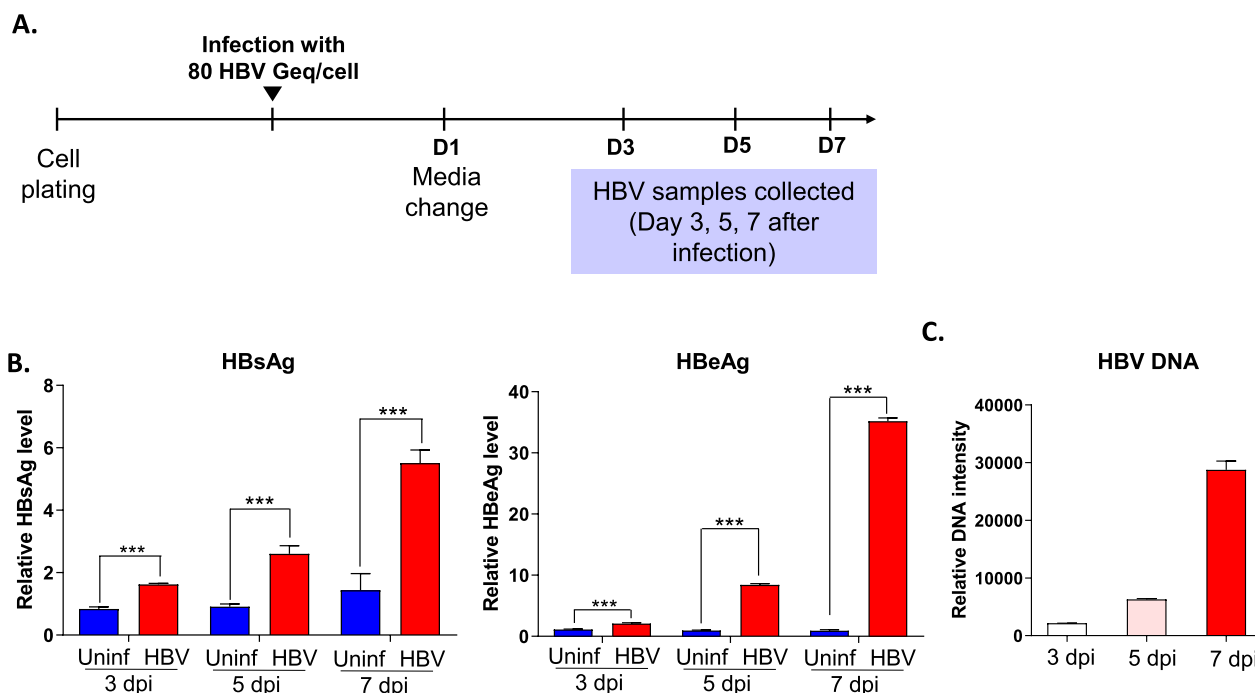

Fig. 1 **A** Workflow for HBV infection. **B** Levels of HBsAg and HBeAg were analyzed by ELISA at the indicated time points. The data compare the antigens secreted from HBV-infected cells (Red bar) and uninfected cells (Blue bar). Statistical significance is indicated (***: *p*-value < 0.001). ELISA data are presented as bar charts (n = 4). **C** Expression of HBV DNA detected by qRT-PCR

(See figure on next page.)
Fig. 2 Expression patterns of 149 genes showing significant dynamic changes. **A** Expression patterns over time in HBV-infected cells. Expression levels were normalized for each gene and then used as input to the heatmap. **B**, **C** Boxplots showing the differences between HBV-infected and uninfected groups for patterns of decrease and increase. The expression patterns of the two groups were compared by date. **D** Scatter plot with R^2 as the y-axis and the fold change at day 7 after infection as the x-axis. Fold change was defined as the average expression level in HBV-infected cells divided by the average expression level in uninfected cells. Green or orange indicates genes with 1.5-fold decreased or increased expression levels, respectively, in HBV-infected cells compared with those in uninfected cells. (E) Expression levels over time for representative genes exhibiting distinct patterns, as determined by RNA-seq data analysis. Genes shown display more than a 1.5-fold difference in expression levels between HBV-infected and uninfected groups at indicated time points
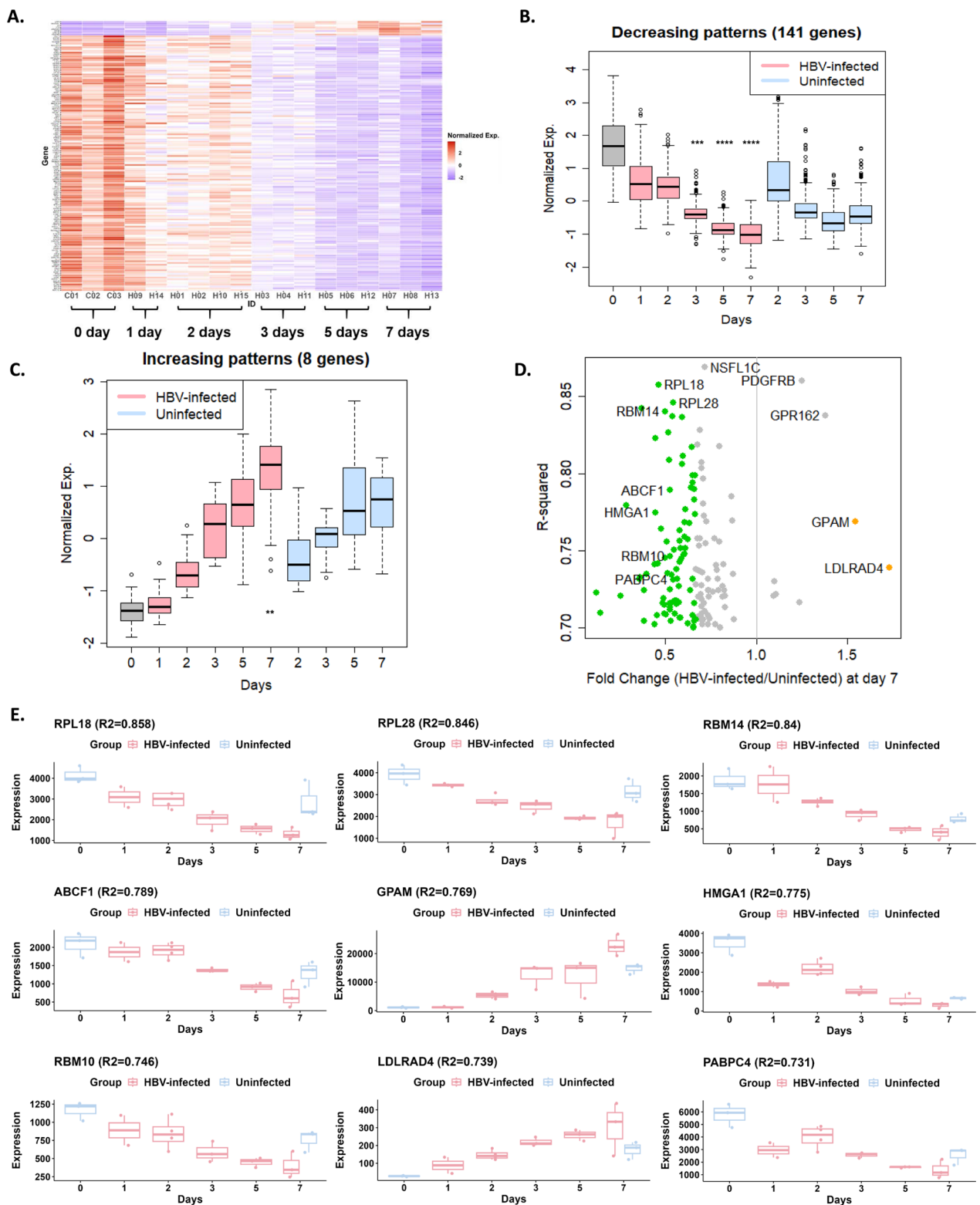
Fig. 2 (See legend on previous page.)

of decrease or increase in the expression patterns of these 149 genes was more pronounced in HBV-infected cells compared to uninfected controls (Supplementary Fig. 1). Specifically, our analysis revealed that while both decreasing and increasing expression patterns were observed in uninfected controls over the 7 day period, the magnitude of these changes was significantly greater in HBV-infected cells (Supplementary Fig. 1B). These findings highlight the distinct expression dynamics induced by HBV infection.

Gene expression patterns in HBV-infected cells exhibited notable and statistically significant differences 3–7 dpi. Notably, by 7 dpi, over half of the genes (58%) displayed a 1.5-fold decrease or increase in expression in HBV-infected cells than in uninfected cells. The scatter plot illustrates both upregulated and downregulated genes across all datasets (Fig. 2D). The most significantly downregulated genes included *RPL18*, *RPL28*, *RBM14*, *ABCF1*, *HMGA1*, *RBM10*, and *PABPC4*, whereas the corresponding upregulated genes consisted of *GPAM* and *LDLRAD4*.

Cross-dataset validation and analysis of HBV-associated gene expression patterns

To prevent bias toward HBV-associated genes specific to one dataset, we conducted a cross-dataset validation analysis using the GSE72068 dataset, mirroring the study design. We focused on the patterns observed in 149 genes that exhibited statistical significance in the main dataset generated through RNA-Seq experiments in this study. Among the 149 genes, there were 112 genes in the GSE72068 dataset (Fig. 3A–C). Within the GSE72068 dataset, the expression of 112 genes showed distinct patterns of decreases or increases in HBV-infected cells, whereas no discernible patterns emerged in uninfected cells over time (Fig. 3D, E). Despite the clear temporal patterns observed in the HBV-infected cells, differences were observed in the gene composition of each pattern. Specifically, 51 of the 112 genes displayed consistent expression patterns in both datasets (Fig. 3B, C). Relative to the expression levels measured 4 h after HBV infection, the expression levels of these 51 genes began to exhibit significant differences starting from the 6 dpi ($p = 2.7 \times 10^{-7}$ for the decreasing pattern and $p = 0.0047$ for the increasing pattern). Notably, the degree of expression reduction between HBV-infected and uninfected cells began to display statistically significant differences at 12 dpi (Fig. 3F). Although the R^2 values for the 51 genes were relatively modest, *RPL28* and *GPAM* emerged among the top genes in terms of fold change (FC), which was consistent with the findings from the primary dataset (Fig. 3G).

Potential biomarkers selection for HBV-mediated chronic liver disease

Apart from the 51 genes validated using the GSE72068 dataset, a collective of 88 genes has been identified, encompassing 37 genes exhibiting substantial evidence (high R^2 and FC values), signifying potential biomarkers for HBV-associated HCC. Detailed information encompassing the main analysis results for significant 51 genes exhibiting consistent patterns across both datasets, is provided in Table 1. The 37 genes were included in the list of potential biomarkers as they could not be identified in the GSE72068 dataset due to limitations of the designed genes (see Table 2). Notably, these 37 genes had high R^2 and FC values, including *ELOA* ($R^2 = 0.818$) and *LDLRAD4* (FC = 1.730). The DAVID functional analysis revealed that most of these genes, accounting for 80%, are known contributors to protein binding (GO:0005515; q-value = 0.0133). Within this subset, 6 genes, including *RPL28*, correspond to the structural elements of ribosomes (hsa03010, q-value = 0.0341). Additionally, among the statistically significant functional pathways and gene ontology terms, we focused on RNA-binding proteins (RBPs, GO:0003723, q-value = 5.6×10^{-4}). Among the 88 genes, 21 (24%) were identified as RBPs, which were downregulated in HBV-infected cells relative to uninfected cells. While previously reported RBPs have shown associations with prognostic markers in HCC patients, regardless of chronic HBV infection, differences exist between these RBPs and the biomarkers identified in this study [13, 14]. Validation experiments employing qRT-PCR were conducted for 21 genes, resulting in the validation of 6 genes (*ABCF1*, *HMGA1*, *RPL28*, *RBM10*, *RBM14*, and *PABPC4*) (Fig. 4B, C). Interestingly, *RBM14* and *RPL28* exhibited a trend of downregulation in HBV-infected PHH and in HCC tumor tissue based on the GSE72068 and GSE25097 datasets (Fig. 4D, E). These findings, supported by evidence from HCC tumor samples, suggest the potential of RBM14 and RPL28 as biomarkers for HBV-associated HCC. As for RBM10, while not prominently highlighted in the GSE72068 and GSE25097 datasets, it had previously been identified as a downregulated tumor suppressor gene in HCC tissues through qRT-PCR [15].

Discussion

HBV is a non-cytopathic, hepatotropic virus known for causing persistent infections that may lead to cirrhosis and HCC. Consequently, numerous studies have focused on characterizing the altered gene expression profiles in host cells following HBV infection [16–18]. Despite extensive research on gene expression changes to understand HBV infection in tumor-derived cell lines
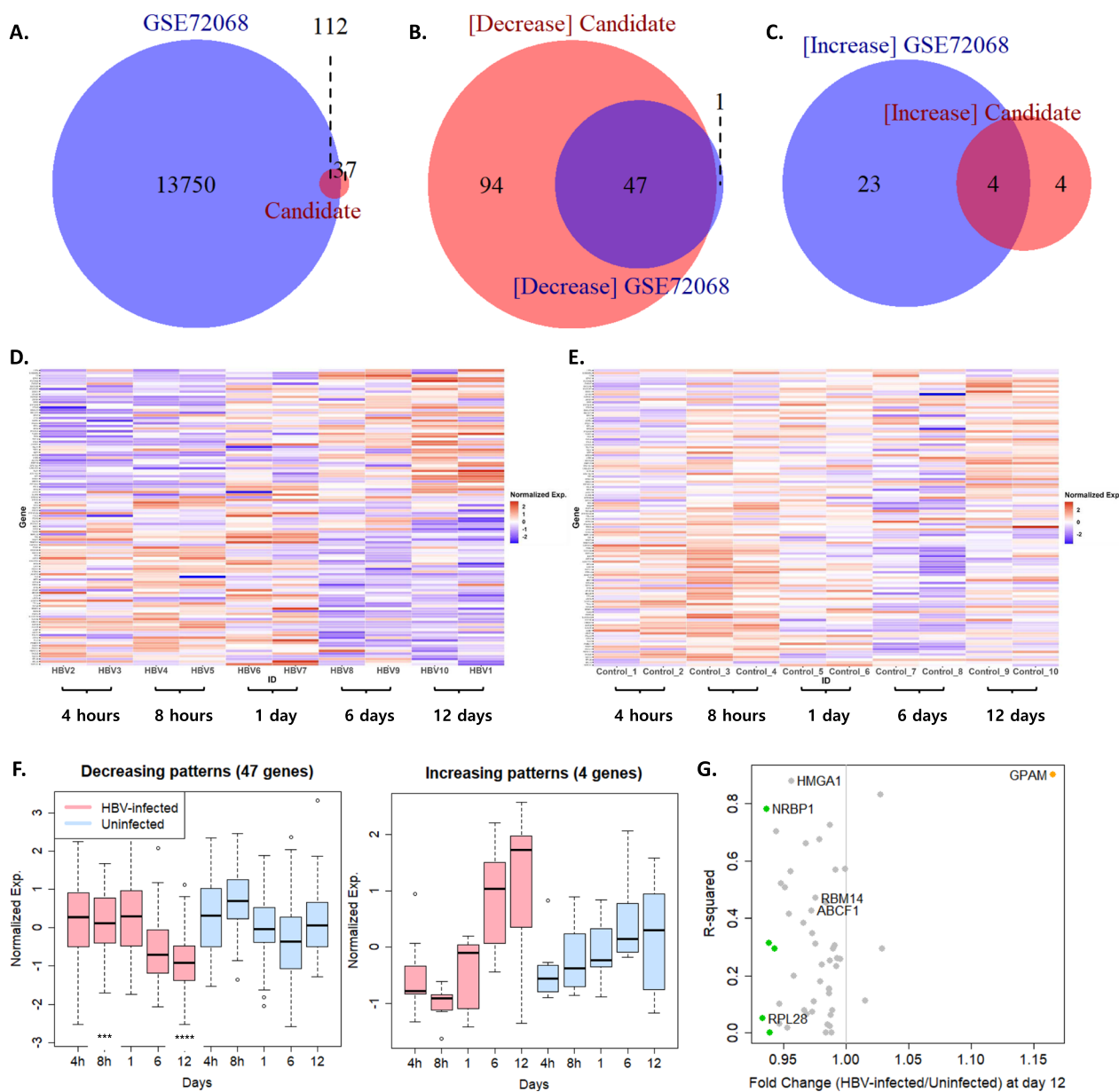
Fig. 3 Expression patterns for 149 genes in the GSE72068 dataset. **A** Venn diagram showing the relationship between the 149 candidate genes in the main dataset and the designed genes in the GSE72068 dataset. **B** Venn diagram showing the number of genes with a decreasing pattern for each dataset around 112 candidate genes. **C** Venn diagram showing the number of genes with an increasing pattern for each dataset around 112 candidate genes. **D**, **E** Expression pattern over time for 112 genes in HBV-infected and uninfected cells in the GSE72068 dataset. Expression levels were normalized for each gene and then used as input for the heatmap. The order of the genes is the same. **F** Boxplots showing the differences between HBV-infected and uninfected groups for both patterns. We focused on 51 genes that showed common patterns with the main dataset. The expression patterns of the two groups were compared by date. **G** Scatter plot with R^2 as the y-axis and the fold change at day 12 after infection as the x-axis. Fold change was defined as the average expression level in HBV-infected cells divided by the average expression level in uninfected cells. Green or orange indicates genes with 1.1-fold decreased or increased expression levels, respectively, in HBV-infected cells compared with those in uninfected cells

and hepatocyte, little is known about HBV infection in PHHs. Our study aimed to identify potential biomarkers for functionally curing HBV infection through a comprehensive understanding of the genes and pathways involved in HBV replication/transcription in PHHs. These cells used to cryopreserve PHHs in this study represent a physiologically relevant in vitro culture system for studying HBV infection. They closely mimic

Hwangbo *et al. Virology Journal*   (2024) 21:170

Page 8 of 12

Table 1 Detailed results of main dataset analysis for genes with common patterns

Gene	Transcript	Coefficient	R^2	*p* value	q-value	Fold change
NSFL1C	NM_016143	− 326.6	0.869	1.8E−08	2.1.E−04	0.716
PDGFRB	NM_002609	206.4	0.860	3.1E−08	2.1.E−04	1.248
RPL18	NM_000979	− 571.9	0.858	3.5E−08	2.1.E−04	0.461
RPL28	**NM_000991**	**− 448.7**	**0.846**	**6.8E−08**	**2.1.E−04**	**0.541**
RBM14	**NM_006328**	**− 326.0**	**0.840**	**8.9E−08**	**2.1.E−04**	**0.500**
DAGLB	NM_139179	− 675.0	0.837	1.0E−07	2.1.E−04	0.538
PRPS1L1	NM_175886	− 61.1	0.836	1.1E−07	2.1.E−04	0.593
PSMC4	NM_006503	− 801.2	0.826	1.8E−07	2.6.E−04	0.518
DUSP1	NM_004417	− 1802.3	0.819	2.5E−07	2.8.E−04	0.675
ELL3	NM_025165	− 48.6	0.803	4.8E−07	3.5.E−04	0.696
USP42	NM_032172	51.2	0.797	6.4E−07	4.1.E−04	0.708
POLE3	NM_017443	− 195.7	0.790	8.3E−07	4.6.E−04	0.656
ABCF1	**NM_001025091**	**− 303.7**	**0.789**	**8.5E−07**	**4.6.E−04**	**0.526**
CALCB	NM_000728	− 21.7	0.779	1.2E−06	5.7.E−04	0.286
HMGA1	**NM_145899**	**− 598.8**	**0.775**	**1.5E−06**	**6.3.E−04**	**0.446**
KDM1B	NM_153042	− 115.7	0.774	1.5E−06	6.4.E−04	0.664
SLC25A19	NM_021734	− 82.0	0.770	1.7E−06	6.8.E−04	0.869
PRPF4	NM_004697	− 236.8	0.769	1.8E−06	6.8.E−04	0.727
GPAM	NM_020918	4192.9	0.769	1.8E−06	6.8.E−04	1.544
GBA2	NM_020944	− 410.5	0.763	2.2E−06	7.6.E−04	0.577
BRMS1	NM_015399	− 69.5	0.757	2.7E−06	8.2.E−04	0.621
RNF25	NM_022453	− 51.2	0.756	2.8E−06	8.2.E−04	0.577
DUSP14	NM_007026	− 228.9	0.751	3.2E−06	8.6.E−04	0.607
LAS1L	NM_031206	− 151.3	0.745	3.9E−06	9.4.E−04	0.497
TTC4	NM_004623	− 169.3	0.742	4.4E−06	1.0.E−03	0.460
MED26	NM_004831	− 39.4	0.741	4.5E−06	1.0.E−03	0.817
AP4B1	NM_006594	− 99.7	0.737	5.2E−06	1.0.E−03	0.686
MTF1	NM_005955	− 213.3	0.732	6.1E−06	1.0.E−03	0.785
FUS	NM_004960	− 356.0	0.727	7.0E−06	1.1.E−03	0.575
AKAP13	NM_007200	− 991.3	0.727	7.0E−06	1.1.E−03	0.816
LSG1	NM_018385	− 292.7	0.724	7.6E−06	1.1.E−03	0.821
RPS5	NM_001009	− 915.6	0.724	7.6E−06	1.1.E−03	0.384
C5	NM_001735	1374.6	0.722	8.1E−06	1.1.E−03	1.107
EID3	NM_001008394	− 38.4	0.720	8.6E−06	1.1.E−03	0.740
RRP12	NM_015179	− 570.5	0.718	9.2E−06	1.1.E−03	0.552
LRP4	NM_002334	28.3	0.717	9.4E−06	1.1.E−03	1.237
CCDC86	NM_024098	− 190.4	0.716	9.5E−06	1.1.E−03	0.540

Results are listed in descending order of R^2. To make it easier to understand at a glance, we have listed the results for genes with R$^2 \geq 0.716$. The coefficient, R^2, *p*-value and q-value are the results of fitting a linear regression model. Fold change was defined as the average expression level in HBV-infected cells divided by the average expression level in uninfected cells, measured at 7 days post-infection. Genes validated through qRT-PCR experiments are indicated in bold

the characteristics of HBV-infected human hepatocytes [19].

In the HBV life cycle, HBV enters hepatocytes by binding to specific receptors on their surface. Once inside, the uncoated viral genome enters the nucleus, forming cccDNA, which acts as a template for viral transcript synthesis. Viral transcription driven by promoter and enhancer regions (ENI and ENII) generates four unspliced viral RNAs − 3.5, 2.4, 2.1, and 0.7 kb − among which the 3.5 kb RNA contains precore and pregenomic RNA species. Notably, the precore mRNA encodes the precore antigen (HBeAg), while the pregenomic RNA directs the translation of the core antigen (HBcAg) and polymerase. After encapsidation, pregenomic RNA serves as a reverse transcription template. Assembled HBV virions are secreted from hepatocytes. Each step

Hwangbo *et al. Virology Journal*   (2024) 21:170

Page 9 of 12

Table 2 Detailed results from analysis of main dataset for undesigned genes in GSE72068 set

Gene	Transcript	Coefficient	R^2	*p* value	q-value	Fold change
ELOA	NM_003198	− 628.2	0.818	2.6E−07	2.8.E−04	0.795
TMEM208	NM_014187	− 182.1	0.806	4.3E−07	3.3.E−04	0.592
LRRC75A	NM_207387	− 187.6	0.799	5.8E−07	4.0.E−04	0.650
TTI2	NM_025115	− 97.5	0.773	1.6E−06	6.5.E−04	0.712
RPLP0	NM_053275	− 7236.4	0.759	2.5E−06	8.2.E−04	0.606
RMC1	NM_013326	− 209.4	0.758	2.6E−06	8.2.E−04	0.771
FNBP1	NM_001363755	− 59.1	0.758	2.6E−06	8.2.E−04	0.690
SRPRB	NM_001379313	− 594.6	0.756	2.8E−06	8.2.E−04	0.795
URB2	NM_014777	− 199.5	0.751	3.3E−06	8.7.E−04	0.545
BRPF1	NM_001003694	− 73.5	0.747	3.7E−06	9.3.E−04	0.600
RBM10	**NM_005676**	**− 157.1**	**0.746**	**3.8E−06**	**9.4E−04**	**0.524**
MEA1	NM_001318942	− 146.7	0.742	4.3E−06	9.9.E−04	0.578
RPL8	NM_000973	− 2073.6	0.741	4.5E−06	1.0.E−03	0.441
GEMIN5	NM_001252156	− 151.7	0.740	4.6E−06	1.0.E−03	0.780
LDLRAD4	NM_181481	55.9	0.739	4.9E−06	1.0.E−03	1.730
EMSY	NM_020193	− 28.0	0.738	5.0E−06	1.0.E−03	0.562
PARP2	NM_001042618	− 98.8	0.738	5.0E−06	1.0.E−03	0.669
FLAD1	NM_025207	− 224.2	0.736	5.4E−06	1.0.E−03	0.512
C2orf81	NM_001145054	− 64.7	0.735	5.5E−06	1.0.E−03	0.395
TMEM265	NM_001256829	− 81.0	0.733	5.9E−06	1.0.E−03	0.359
KANSL2	NM_017822	− 72.2	0.732	6.0E−06	1.0.E−03	0.651
CFAP73	NM_001144872	− 48.0	0.732	6.1E−06	1.0.E−03	0.357
PABPC4	**NM_001135653**	**− 828.8**	**0.731**	**6.1E−06**	**1.0.E−03**	**0.545**
CFH	NM_000186	4273.6	0.730	6.3E−06	1.0.E−03	1.100
MIEF1	NM_019008	− 295.5	0.724	7.5E−06	1.1.E−03	0.638
CSRNP1	NM_033027	− 153.0	0.722	8.2E−06	1.1.E−03	0.695
COPS8	NM_006710	− 207.6	0.720	8.4E−06	1.1.E−03	0.828
MAP3K4	NM_001291958	− 168.2	0.717	9.2E−06	1.1.E−03	0.559
USP2	NM_171997	− 34.8	0.716	9.6E−06	1.1.E−03	0.525
ATRIP	NM_130384	− 66.0	0.711	1.1E−05	1.2.E−03	0.718
BUD23	NM_001202560	− 179.0	0.707	1.2E−05	1.3.E−03	0.583
SMIM29	NM_001008703	− 51.9	0.707	1.3E−05	1.3.E−03	0.576
ZBTB43	NM_001135776	− 212.8	0.706	1.3E−05	1.3.E−03	0.744
ZBTB21	NM_020727	− 178.4	0.705	1.3E−05	1.3.E−03	0.876
URGCP	NM_001077664	− 298.7	0.705	1.3E−05	1.3.E−03	0.528
ODC1	NM_001287188	− 2034.3	0.705	1.3E−05	1.3.E−03	0.381
GPAT3	NM_032717	− 121.6	0.700	1.5E−05	1.4.E−03	0.652

Results are listed in descending order of R^2. The coefficient, R^2, *p*-value and q-value are the results of fitting a linear regression model. Fold change was defined as the average expression level in HBV-infected cells divided by the average expression level in uninfected cells, measured at 7 days post-infection. Genes validated through qRT-PCR experiments are indicated in bold

of the HBV life cycle is heavily dependent on the host factors, such as hepatocyte-enriched and ubiquitous transcription factors, regulating viral replication and transcription via promoter and enhancer regions. Therefore, we focused on changes in gene expression and transcription dynamics of hepatocyte related with HBV replication/transcription processes after HBV infection. Our analysis suggests significant changes primarily in RNA metabolism-related genes within PHHs depending on the time following HBV infection.

HBV directly alters RNA metabolism by interacting with cellular RBPs, affecting RNA processing and stability in host cell [20]. A study by Chabrolles et al. revealed that HBV core protein was found to interact with RBPs, notably SRSF10. Their functional studies identified SRSF10 as the HBV RNA regulator primarily
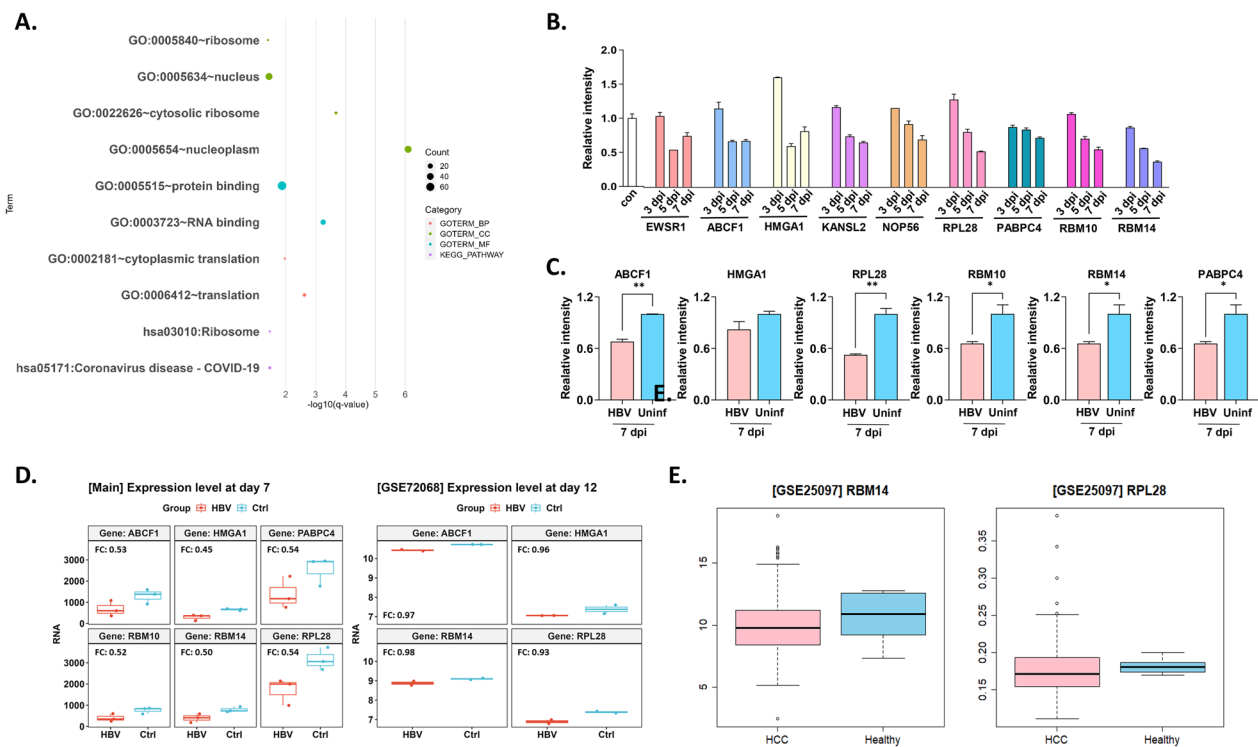
Hwangbo *et al. Virology Journal*   (2024) 21:170

Page 10 of 12

Fig. 4 Functional enrichment analysis and qRT-PCR-based validation analysis. **A** All statistically significant enriched terms are displayed (q-value < 0.05). The count indicates the number of genes belonging to each term. **B**, **C** The quantitative analysis of genes identified by qRT-PCR. Relative expression levels were calculated by normalizing β-actin expression. Significant differences between uninfected and HBV-infected primary human hepatocytes at 7 dpi are represented (*$p < 0.05$, **$p < 0.01$). **D** Comparison of expression levels between two groups on the last day of measurement for each dataset. Fold change (FC) is defined as the average RNA expression level in the HBV group divided by that in the control (Ctrl) group. (E) Two genes validated in the GSE25097 dataset show downregulated expression levels in real HCC samples compared with those in healthy liver samples

in its dephosphorylated state within infected cell nuclei, influencing nascent HBV RNA levels without affecting HBV RNA splicing [21]. Additionally, virus-induced changes in cell environment indirectly impact RNA metabolism, leading to dysregulated gene expression and altered mRNA levels crucial for immune responses, cell functions, and apoptosis during HBV infection [22–24]. In this study, we identified six RNA metabolism-associated genes involved in HBV infection, such as *ABCF1, HMGA1, RPL28, RBM10, RBM14, and PABPC4.* They were successfully validated through qRT-PCR experiments and analysis of two separate datasets. Notably, *RBM14* and *RPL28* were involved in hepatocarcinogenesis and used as potential biomarkers for HBV associated HCC [25, 26]. RBM14 plays diverse roles in maintaining the stem-like state of glioblastoma multiforme spheres and assisting PARP-dependent DNA repair at double-strand breaks. Moreover, elevated RBM14 expression in HCC modulate the M2-phenotype polarization of KCs through N-methyladenosine (m6A) methylation regulation, thereby promoting HCC cells' malignant aggressiveness [27].

RPL28 is implicated in HCC by modulating murine double minute 2 (MDM2), affecting the tumor suppressor p53's function. Its negative regulation of MDM2 inhibits p53 ubiquitination, stabilizing p53's tumor-suppressive role. Dysregulated RPL28 activity in hepatocarcinogenesis may disrupt these processes, potentially facilitating HCC cell growth [28]. However, there is insufficient research on the functions of *RBM14* and *RPL28* related to the HBV infection. Collectively, our results and previous reports suggested that the changed expression of RNA processing regulatory factors in HBV-associated HCC could serve as the potential biomarkers.

In this study, we revealed a modest number of significantly differentially expressed gene between HBV-infected and non-infected PHH. These unexpected results might be due to the differences in cell viability and metabolic activity of freshly isolated PHHs compared to cryopreserved PHHs due to the preservation stress incurred during freezing and thawing [29, 30]. Therefore, further validations and investigations using more natural models and clinical samples would be necessary in the future. Additional experiments are necessary to

Hwangbo *et al. Virology Journal*   (2024) 21:170

Page 11 of 12

investigate differences in gene expression related to susceptibility to HBV infection in freshly isolated PHHs obtained from different donors.

In summary, our study presents comprehensive transcriptional profiling of HBV infection dynamics, validates the 10 genes related to RNA-metabolism on HBV infection. We utilized the PHHs, which are regarded as the most physiologically relevant in vitro models for studying HBV infection. PHHs closely mirror the characteristics of human liver cells, the primary target of HBV. Our findings uncovered alterations in various genes and cellular pathways linked to mRNA metabolism, alternative splicing, and spliceosomes during HBV replication. Several of these genes are associated with HBV-associated HCC. These findings hint at the potential for identifying novel biomarkers to address HBV-associated HCC.

Conclusions
Our study delineated alterations in gene expression within PHHs caused by HBV infection. We pinpointed RBPs crucial in mRNA metabolism and the regulation of alternative splicing during HBV infection. Grasping the functional roles of host factor networks in HBV infection holds promise in elucidating the molecular mechanisms behind HBV replication/transcription and could pave the way for developing therapeutic interventions against HBV infection.

Supplementary Information
The online version contains supplementary material available at https://doi.org/10.1186/s12985-024-02446-3.

Supplementary Material 1.

Supplementary Fig. 1. Expression patterns of 149 genes in uninfected cells compared with HBV-infected cells. (A) Expression patterns over time in uninfected cells. Expression levels were normalized for each gene and used as input for the heatmap. (B, C) Violin plots depicting differences between HBV-infected and uninfected groups on days 0 and 7. Significant differences between the two group are indicated (**P < 0.01, ***P<0.001, and ****P<1×10-15).

Author contributions
Experiments were conceived and designed by W.H., J.Y.R. and mainly performed by G.K. and S.H. Data were processed and analyzed by S.H. The original draft was Written by G.K. The manuscript was reviewed and supervised by Y.C., Y.K.P. and S.B. All authors have read and agreed to the published version of the manuscript.

Funding

Availability of data and materials
The main datasets we generated in this study are available in Additional File 1. The two validation datasets can be download from the GEO database. (https://www.ncbi.nlm.nih.gov/gds). GEO accession ID: GSE72068: https://www.ncbi.nlm.nih.gov/geo/query/acc.cgi?acc=GSE72068, GSE25097: https://www.ncbi.nlm.nih.gov/geo/query/acc.cgi?acc=GSE25097.

Declarations

Competing interests
The authors declare no competing interests.

Author details
[1]Department of Genomic Medicine, Seoul National University Hospital, 101 Daehak-ro, Jongno-gu, Seoul 03080, Korea. [2]Division of Chronic Viral Diseases, Center for Emerging Virus Research, Korea National Institute of Health, 187 Osongsaengmyeong 2-ro, Cheongju 363951, Korea. [3]Department of Biotechnology, Duksung Women's University, Seoul 01369, Korea. [4]Department of Pharmacy, Chungbuk National University, Cheongju 28644, Korea.

References
1. Lamontagne J, Mell JC, Bouchard MJ. Transcriptome-wide analysis of hepatitis B virus-mediated changes to normal hepatocyte gene expression. PLoS Pathog. 2016;12(2):e1005438.
2. Wong MCS, Huang JLW, George J, Huang J, Leung C, Eslam M, et al. The changing epidemiology of liver diseases in the Asia-Pacific region. Nat Rev Gastroenterol Hepatol. 2019;16(1):57–73.
3. Dandri M, Petersen J. cccDNA maintenance in chronic hepatitis B—targeting the matrix of viral replication. Infect Drug Resist. 2020;13:3873–86.
4. Bar-Yishay I, Shaul Y, Shlomai A. Hepatocyte metabolic signalling pathways and regulation of hepatitis B virus expression. Liver Int. 2011;31(3):282–90.
5. Ito N, Nakashima K, Sun S, Ito M, Suzuki T. Cell type diversity in hepatitis B virus RNA splicing and its regulation. Front Microbiol. 2019;10:207.
6. Lee HW, Choi Y, Lee AR, Yoon CH, Kim KH, Choi BS, et al. Hepatocyte growth factor-dependent antiviral activity of activated cdc42-associated kinase 1 against hepatitis B virus. Front Microbiol. 2021;12:800935.
7. Lee DH, Lee HJ, Lee YJ, Kang HM, Jeong OM, Kim MC, et al. DNA barcoding techniques for avian influenza virus surveillance in migratory bird habitats. J Wildl Dis. 2010;46(2):649–54.
8. Ambardar S, Gupta R, Trakroo D, Lal R, Vakhlu J. High throughput sequencing: an overview of sequencing chemistry. Indian J Microbiol. 2016;56(4):394–404.
9. Yeo SJ, Than DD, Park HS, Sung HW, Park H. Molecular characterization of a novel avian influenza A (H2N9) strain isolated from wild duck in Korea in 2018. Viruses. 2019;11(11):1046.
10. Langmead B, Salzberg SL. Fast gapped-read alignment with Bowtie 2. Nat Methods. 2012;9(4):357–9.
11. Ancey PB, Testoni B, Gruffaz M, Cros MP, Durand G, Le Calvez-Kelm F, et al. Genomic responses to hepatitis B virus (HBV) infection in primary human hepatocytes. Oncotarget. 2015;6(42):44877–91.
12. Sherman BT, Hao M, Qiu J, Jiao X, Baseler MW, Lane HC, et al. DAVID: a web server for functional enrichment analysis and functional annotation of gene lists (2021 update). Nucleic Acids Res. 2022;50(W1):W216–21.
13. Li M, Liu Z, Wang J, Liu H, Gong H, Li S, et al. Systematic analysis identifies a specific RNA-binding protein-related gene model for prognostication and risk-adjustment in HBV-related hepatocellular carcinoma. Front Genet. 2021;12:707305.
14. Lin Y, Liang R, Qiu Y, Lv Y, Zhang J, Qin G, et al. Expression and gene regulation network of RBM8A in hepatocellular carcinoma based on data mining. Aging (Albany NY). 2019;11(2):423–47.
15. Zhao Z, Li J, Shen F. Protective effect of the RNA-binding protein RBM10 in hepatocellular carcinoma. Eur Rev Med Pharmacol Sci. 2020;24(11):6005–13.

Hwangbo *et al. Virology Journal*   (2024) 21:170

Page 12 of 12

16. Liao X, Yu T, Yang C, Huang K, Wang X, Han C, et al. Comprehensive investigation of key biomarkers and pathways in hepatitis B virus-related hepatocellular carcinoma. J Cancer. 2019;10(23):5689–704.

17. Xie S, Jiang X, Zhang J, Xie S, Hua Y, Wang R, et al. Identification of significant gene and pathways involved in HBV-related hepatocellular carcinoma by bioinformatics analysis. PeerJ. 2019;7:e7408.

18. Yang Y, Zhong Z, Ding Y, Zhang W, Ma Y. Zhou L Bioinformatic identification of key genes and pathways that may be involved in the pathogenesis of HBV-associated acute liver failure. Genes Dis. 2018;5(4):349–57.

19. Hu J, Lin YY, Chen PJ, Watashi K, Wakita T. Cell and animal models for studying hepatitis B virus infection and drug development. Gastroenterology. 2019;156(2):338–54.

20. Zhang T, Zheng H, Lu D, Guan G, Li D, Zhang J, et al. RNA binding protein TIAR modulates HBV replication by tipping the balance of pgRNA translation. Signal Transduct Target Ther. 2023;8(1):346.

21. Chabrolles H, Auclair H, Vegna S, Lahlali T, Pons C, Michelet M, et al. Hepatitis B virus Core protein nuclear interactome identifies SRSF10 as a host RNA-binding protein restricting HBV RNA production. PLoS Pathog. 2020;16(11):e1008593.

22. Jose-Abrego A, Roman S, Laguna-Meraz S, Panduro A. Host and HBV interactions and their potential impact on clinical outcomes. Pathogens. 2023;12(9):1146.

23. Wang S, Gao S, Ye W, Li Y, Luan J, Lv X. The emerging importance role of m6A modification in liver disease. Biomed Pharmacother. 2023;162:114669.

24. Yang Y, Yan Y, Yin J, Tang N, Wang K, Huang L, et al. O-GlcNAcylation of YTHDF2 promotes HBV-related hepatocellular carcinoma progression in an N(6)-methyladenosine-dependent manner. Signal Transduct Target Ther. 2023;8(1):63.

25. Sun T, Zhu W, Ru Q, Zheng Y. Silencing RPL8 inhibits the progression of hepatocellular carcinoma by down-regulating the mTORC1 signalling pathway. Hum Cell. 2023;36(2):725–37.

26. Zhang Z, Gao W, Liu Z, Yu S, Jian H, Hou Z, et al. Comprehensive analysis of m6A regulators associated with immune infiltration in Hepatitis B virus-related hepatocellular carcinoma. BMC Gastroenterol. 2023;23(1):259.

27. Hu J, Yang L, Peng X, Mao M, Liu X, Song J, et al. METTL3 promotes m6A hypermethylation of RBM14 via YTHDF1 leading to the progression of hepatocellular carcinoma. Hum Cell. 2022;35(6):1838–55.

28. Shi Y, Wang X, Zhu Q, Chen G. The ribosomal protein L28 gene induces sorafenib resistance in hepatocellular carcinoma. Front Oncol. 2021;11:685694.

29. Hengstler JG, Utesch D, Steinberg P, Platt KL, Diener B, Ringel M, et al. Cryopreserved primary hepatocytes as a constantly available in vitro model for the evaluation of human and animal drug metabolism and enzyme induction. Drug Metab Rev. 2000;32(1):81–118.

30. Illouz S, Alexandre E, Pattenden C, Mark L, Bachellier P, Webb M, et al. Differential effects of curcumin on cryopreserved versus fresh primary human hepatocytes. Phytother Res. 2008;22(12):1688–91.

Publisher's Note